Effect of Viscosity on Mechanics of Single, Skinned Fibers from Rabbit Psoas Muscle

P. Bryant Chase, Todd M. Denkinger, and Martin J. Kushmerick
Departments of Radiology, Physiology and Biophysics, and Bioengineering, University of Washington, Seattle, Washington 98195 USA

ABSTRACT Muscle contraction is highly dynamic and thus may be influenced by viscosity of the medium surrounding the myofilaments. Single, skinned fibers from rabbit psoas muscle were used to test this hypothesis. Viscosity within the myofilament lattice was increased by adding to solutions low molecular weight sugars (disaccharides sucrose or maltose or monosaccharides glucose or fructose). At maximal Ca^{2+} activation, isometric force (F_i) was inhibited at the highest solute concentrations studied, but this inhibition was not directly related to viscosity. Solutes readily permeated the filament lattice, as fiber diameter was unaffected by added solutes (except for an increased diameter with $F_i < 30\%$ of control). In contrast, there was a linear dependence upon 1/viscosity for both unloaded shortening velocity and also the kinetics of isometric tension redevelopment; these effects were unrelated to either variation in solution osmolarity or inhibition of force. All effects of added solute were reversible. Inhibition of both isometric as well as isotonic kinetics demonstrates that viscous resistance to filament sliding was not the predominant factor affected by viscosity. This was corroborated by measurements in relaxed fibers, which showed no significant change in the strain-rate dependence of elastic modulus when viscosity was increased more than twofold. Our results implicate cross-bridge diffusion as a significant limiting factor in cross-bridge kinetics and, more generally, demonstrate that viscosity is a useful probe of actomyosin dynamics.

INTRODUCTION

Active muscle contraction is a highly dynamic process at both the macroscopic and particularly at the microscopic level (Finer et al., 1994; Huxley and Simmons, 1971; Molloy et al., 1995; Thomas et al., 1995). Force generation and shortening result from asynchronous, cyclic interactions of myosin with actin coupled to hydrolysis of MgATP (Cooke, 1995). Evidence indicates that during the actomyosin cycle, myosin catalytic domains (subfragment 1 "heads") move from the vicinity of the thick filament toward the thin filament, bind to specific sites on actin, and undergo nucleotide-dependent changes in conformation (Fisher et al., 1995; Harford and Squire, 1992; Huxley, 1969; Yu and Brenner, 1989).

Because of the small size of actin filaments and particularly myosin cross-bridges, the fundamental motions underlying muscle contraction occur in the realm of low Reynolds number, and thus dynamic muscle function might reasonably be predicted to be affected by cytoplasmic viscosity. However, it was suggested in 1924 that the hyperbolic force-velocity relation of intact muscle provided evidence against viscosity being the primary resistive force that opposes unloaded shortening (Gasser and Hill, 1924). The total force exerted on an individual actin filament is the sum of cross-bridge forces and a viscous force (F_η), which is linearly proportional to speed (dx/dt) for simple Newtonian fluids:

$$F_\eta \propto \eta \frac{dx}{dt} \tag{1}$$

where η is the viscosity of the medium. Huxley (1957) suggested that the ensemble of myosin cross-bridges is the main determinant of shortening velocity, not only the driving force for muscle shortening but also the primary resistance, as myosin cross-bridges are mechanically coupled via a common thick filament backbone and the architecture of the sarcomere. In this model, a portion of cross-bridges actively translocating an actin filament also push the remaining bound cross-bridges past the range of useful work, i.e., into a region of negative strain. In support of this view, calculations (assuming cytoplasmic viscosity approximately twice that of water) (Huxley, 1980) and experimental measurements in frog muscle fibers (Bagni et al., 1995; Ford et al., 1977) suggest that the viscous force that opposes filament sliding in a sarcomere shortening at its maximal velocity should be several orders of magnitude smaller than cross-bridge forces measured under isometric conditions (Finer et al., 1994; Molloy et al., 1995). In addition to these possible frictional effects, increased viscosity of the solvent decreases chemical reaction kinetics (Ansari et al., 1992; Beece et al., 1980; Gavish and Werber, 1979; Hunt et al., 1994). Thus viscosity may also affect other fundamental properties of actomyosin interaction such as ATPase kinetics independently of molecular frictional effects and of dynamic sliding of the filaments.

Evidence from skinned fiber experiments suggests that variations in solution viscosity do in fact affect contractile

Received for publication 29 October 1996 and in final form 2 December 1997.

T. M. Denkinger's present address: University of Virginia Health Science Center, Charlottesville, VA.

Address reprint requests to Dr. P. Bryant Chase, University of Washington, Departments of Radiology and Physiology and Biophysics, Box 357115, Seattle, WA 98195-7115. Tel.: 206-543-3499; Fax: 206-543-3495; E-mail: chase@u.washington.edu.

0006-3495/98/03/1428/11 $2.00

performance (Ashley and Moisescu, 1977; Chase and Kushmerick, 1988; Endo et al., 1979). At high concentrations, maximal Ca^{2+}-activated force has been shown to be inhibited by small molecules (sucrose and glucose) that readily permeate the filament lattice of skinned fibers (Ashley and Moisescu, 1977; Chase and Kushmerick, 1988; Endo et al., 1979). Calcium sensitivity was also decreased under these conditions (Endo et al., 1979). Unloaded shortening velocity was inhibited to a greater extent than isometric force (Chase and Kushmerick, 1988), strongly implying (but not proving) that the relevant variable was viscosity as viscosity was not specifically evaluated in the earlier work. Further support derives from the observations of Hunt et al. (1994) who demonstrated that increased solution viscosity slows and can actually stall microtubules translocated by single kinesin molecules in an in vitro motility assay.

To directly evaluate the hypothesis that viscosity within a muscle cell influences its function, we used skinned fiber preparations in which the medium bathing the myofilaments is under direct experimental control. Solution viscosity was varied by adding low molecular weight (MW) sugars (sucrose, maltose, glucose, or fructose); comparing effects of mono- versus disaccharides permitted separation of viscosity effects from effects related to osmotic pressure. The results are consistent with previous suggestions that viscous resistance to filament sliding is not a major factor affecting muscle shortening. Nonetheless, there was a marked viscosity dependence of both the rate of isometric tension redevelopment and also unloaded shortening velocity, which implies a significant modulation of cellular motility by cytoplasmic viscosity, resulting at least in part from viscous effects on cross-bridge diffusion to binding sites on actin. A portion of these results have been reported in abstract form (Chase et al., 1996).

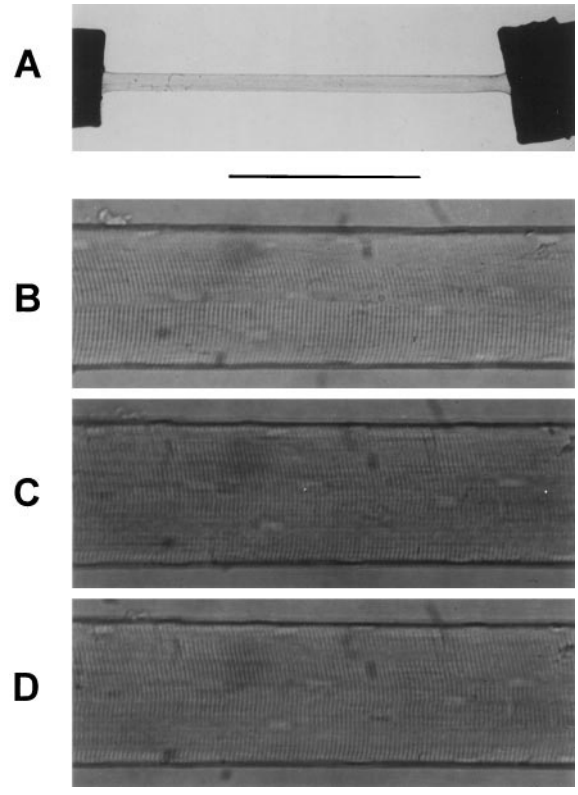

FIGURE 1 Photomicrographs of a single, glycerinated psoas fiber relaxed at pCa 9.2 (*A* and *B*, no added solute) or maximally Ca^{2+}-activated at pCa 4.5 (*C*, no added solute; *D*, 0.4 M sucrose). The fiber was attached to a force transducer and motor by aluminum foil clips (see Materials and Methods), which are visible at either end in *A*. Both ends of the fiber segment were chemically fixed by local application of glutaraldehyde before attaching foil clips (Materials and Methods); approximately 150 μm of fixed segment is visible on either end outside of the clip (*A*), as determined at the end of the experiment (Materials and Methods). L_S was 2.57 μm at pCa 9.2 (*A*); at pCa 4.5, L_S was 2.49 μm (*B*) or 2.48 μm (*C*). The calibration bar represents 830 μm (*A*) or 104 μm (*B–D*).

MATERIALS AND METHODS

Preparation of single, glycerinated fibers

Single fiber segments from rabbit psoas muscle were dissected and prepared for mechanical experiments as described previously (Chase and Kushmerick, 1988; Chase et al., 1994b). In brief, small bundles of psoas muscle, tied to Teflon strips at in vivo length, were removed from adult, New Zealand White rabbits that had been euthanized with pentobarbital (120 mg kg^{-1}) administered through the marginal ear vein. The bundles were treated with 0.5% Brij 58 detergent and then 50% glycerol in skinning solution and were stored at −20°C before use. Fiber segments were dissected in a chilled bath of 50% glycerol/skinning solution with 10 mg ml^{-1} bovine serum albumin or soybean trypsin inhibitor added to protect the fibers against diffusion of fixative. One precaution we took to stabilize fiber structure and mechanical properties during prolonged activation was to chemically fix the ends of the fiber segments by localized microapplication of 5% glutaraldehyde (plus 1 mg ml^{-1} fluorescein for visualization) (Chase and Kushmerick, 1988). The fixed ends were wrapped in aluminum foil T-clips (partially visible in Fig. 1 *A*) for attachment to the mechanical apparatus via small hooks (Chase and Kushmerick, 1988; Chase et al., 1994b).

Microscopy and mechanical apparatus

Fiber segments were mounted on a motor (step time ≤ 300 μs; General Scanning, Watertown, MA) to control overall fiber length at one end and on a capacitative-type force transducer (2.2 kHz resonant frequency; Cambridge Technology, Watertown, MA) at the other end. The motor and force transducer were located on a modified stage of an inverted microscope (Chase and Kushmerick, 1988; Sweeney et al., 1987).

Sarcomere length measurement

Steady-state, isometric values of sarcomere length (L_S) and fiber diameter were measured during an experiment using an optical micrometer and also, after the experiment, from photographic prints (Fig. 1, *B–D*). The length of the unfixed, central portion of the fiber (L_F) was determined at the end of the experiment as described previously (Chase and Kushmerick, 1988; Chase et al., 1994b); note that L_F is shorter than the length of fiber visible between T-clips (L_{tot}; Fig. 1 *A*) as a short fixed region extends beyond the edge of the clips (Chase and Kushmerick, 1988). L_F was 1.55 ± 0.24 mm at relaxed (pCa > 8); L_S = 2.56 ± 0.06 μm (mean ± SD; N = 31). The diameter of relaxed fibers was 75 ± 16 μm (mean ± SD; N = 31). During maximal Ca^{2+} activation (pCa 5–4), L_S decreased to 2.43 ± 0.08 μm (mean ± SD; N = 27, as measurements were not made on four fibers).

In some experimental protocols, L_S was also measured by HeNe laser diffraction during transient length changes as well as during isometric steady state. Each diffraction first-order maximum was compressed using a cylindrical lens, which increased the intensity of light impinging upon the detectors and which summed light intensity from the substructure within each first order, and were continuously monitored as described (Chase et al., 1994a,b, 1993). One first order was sensed by a wide bandwidth Schottky photodetector (model PIN-LSC5D, United Detector Technologies, Hawthorne, CA) whereas the opposite first order was sensed by a photodiode array (model RL0256C/17; Reticon, Sunnyvale, CA) (Iwazumi and Pollack, 1979). L_S signals were recorded and analyzed primarily for protocols that involved small length changes (typically $< 1\%$ L_F), thus minimizing potential artifacts due to translation of sarcomeres (Burton and Huxley, 1995; Goldman, 1987; Rüdel and Zite-Ferenczy, 1979).

Solutions

Skinned fiber solutions were calculated and prepared essentially as described (Chase and Kushmerick, 1988), with slight modifications to adjust solution viscosity. The basic composition of solutions was (in mM): 5 MgATP, 1 Pi, 4 EGTA (pCa 5.0–4.0 (activating) or pCa $>$ 8 (relaxing), 15 PCr, 1 mg ml^{-1} creatine kinase (CK; 260 U ml^{-1}), 100 K^+ plus Na^+, 3 Mg^{2+}, 50 MOPS, and 1 dithiothreitol. Solution pH was adjusted to 7.1 at 12°C. Ionic strength ($\Gamma/2$) was 0.2 M and was adjusted with Tris and acetate.

Experimental solutions were held in 300-μl wells machined in anodized aluminum. The bottom of each well consisted of a glass number 1 coverslip and, for L_S measurement by HeNe laser diffraction, the top was covered with a portion of a plain glass microscope slide. The temperature was 12–15°C (measured with a K-type thermocouple) and was controlled to within 1°C during individual experiments.

No agents for osmotic compression of the filament lattice (e.g., Dextran T-500) were added to solutions because Dextran T-500 at 0.4% (w:v) increased bulk viscosity more than fourfold. As size exclusion maintains the major fraction of Dextran T-500 outside of the filament lattice, it would therefore have less effect on viscosity of the medium within the fiber. Thus it would not be possible to correlate fiber mechanical performance with the actual viscosity of the medium bathing the myofilaments when such high MW osmotic agents were added to the bulk solution.

Solution viscosity

To vary solution viscosity, we used four low MW sugars: disaccharides sucrose and maltose and monosaccharides glucose and fructose. Low MW compounds were used to ensure that solutes would readily permeate the filament lattice of skinned fibers (as verified in Results; see Fig. 5) and thus interfilament viscosity would be the same as bulk solution viscosity, in contrast to high MW compounds (e.g., Dextran T-500) discussed above. These molecules are uncharged and therefore had no effect on $\Gamma/2$, except through a small reduction of water activity (see Fig. 4 in Results).

Sugars were added to solutions in one of two ways, with no significant difference in results obtained using either method. Either 1) solid sugar was dissolved directly in a solution (and any resulting volume change corrected for) or 2) concentrated sugar stock solution was mixed with 2X concentrated fiber solution and water was added to make up the difference in volume. Note that, throughout the text and also in Figs. 2, 4 *A*, 5, and 7 *A*, added solute refers to the concentration of low MW sugars (sucrose, maltose, glucose, or fructose) in fiber solutions beyond standard components.

To directly correlate fiber mechanics with bulk solution viscosity, we used an Ostwald-type viscometer (VWR Scientific, West Chester, PA) to measure the viscosity of fiber solutions relative to that of water. Relative viscosity (η/η_0) was calculated according to:

$$\frac{\eta}{\eta_0} = \frac{t\rho}{t_0\rho_0} \tag{2}$$

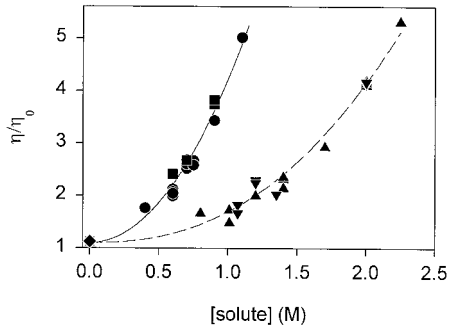

FIGURE 2 Increase of solution viscosity by low molecular weight sugars (sucrose, ●; maltose, ■; glucose, ▲; fructose, ▼). Relative viscosity (η/η_0) of experimental solutions, relative to water, was determined at 12°C (Materials and Methods). Points represent individual measurements except for control solutions with no added solute (◆), which is shown as mean ± SD ($N = 24$). Lines were drawn according to the nonlinear least squares regressions using Eq. 3 for disaccharides (—) or monosaccharides (- - -).

where t is the flow time measured in the viscometer, ρ is density, and the subscript 0 indicates measurements on water (McKie and Brandts, 1972). All viscosity measurements, including that of water, were made at the experimental temperature (12°C) by immersing the viscometer in a temperature-controlled, circulating water bath.

The viscosity of control fiber solutions (no added sugars) was slightly greater than that of deionized water at the same temperature (12°C), $\eta/\eta_0 = 1.12 \pm 0.08$ (mean ± SD; $N = 24$; Fig. 2), due to the presence of solutes other than sugars (salts, buffers, etc.). Addition of low MW sugars increased η/η_0 as expected (Fig. 2) (Weast, 1982). To obtain similar increases of η/η_0 for the various sugars used, it was necessary to add approximately twofold higher concentrations of monosaccharides than disaccharides (compare the two curves in Fig. 2) over the range used in these experiments (Weast, 1982). To estimate η/η_0 in experimental solutions as a function of added solute, we used nonlinear least-squares regression to fit the data for mono- and disaccharides separately to the following expression:

$$\frac{\eta([\text{solute}])}{\eta_0} = A[\text{solute}]^B + \frac{\eta(0)}{\eta_0} \tag{3}$$

where A and B were the fitted parameters. In Eq. 3, $\eta(0)/\eta_0$ was constrained to be equal to the average value of η/η_0 measured in the absence of added solute (see above).

Experimental control, data acquisition, and data analysis

During the course of these experiments, two different computer systems were employed for experimental control, data acquisition, and analysis. In earlier experiments, a PDP-11/23 system (Digital Equipment, Maynard, MA) with custom data acquisition hardware and software was used (Chase and Kushmerick, 1988; Sweeney et al., 1987). In later experiments, a PC-based system with a DT2831-G board (Data Translation, Marlboro, MA) and custom software were used (Chase et al., 1994a,b).

Fiber stabilization

In addition to chemical fixation of fiber segment ends and reduced temperature as methods of maintaining integrity of fiber structure and mechanical properties during prolonged activation, both experimental control systems also employed periodic (0.2 Hz) unloading (i.e., fiber shortening followed by restretch to the isometric length) (Brenner, 1983; Chase and Kushmerick, 1988; Sweeney et al., 1987). Periodic length releases and the

corresponding force transients are visible as vertical lines in both traces of the slow time base recording of Fig. 3. Notable in Fig. 3 is the stability of force throughout >14 min of maximal Ca^{2+} activation. Fig. 1, *C* and *D*, illustrate structural stability of the sarcomere striation pattern at maximal Ca^{2+} activation (compare with Fig. 1 *B*), both in the absence (Fig. 1 *C*) and presence (Fig. 1 *D*) of low MW sugars.

Determination of isometric force

Steady-state, isometric force (F_i) at maximal Ca^{2+} activation (pCa 5–4) was determined from the initial portion of digitized records such as those shown in Fig. 6, *A* and *B*. Note that the force baseline (dotted lines in Fig. 6, *A* and *B*) could be unambiguously determined from such records during the period of unloaded shortening. F_i in control conditions (♦ in Fig. 4) was 145 ± 38 mN mm^{-2} (mean ± SD; $N = 31$). Passive tension obtained in a similar manner at pCa > 8 was 2 ± 2% of F_i (mean ± SD; $N = 27$; determinations were not made on four fibers). For comparison between fibers, F_i at elevated η/η_0 was normalized to the average of bracketing control determinations (♦ in Fig. 4; also see Fig. 3).

Velocity of unloaded shortening and maximal velocity of shortening

The majority of measurements of velocity of unloaded shortening (V_{US}) were made using the slack method (Edman, 1979). A series of up to nine length steps were applied to the fiber (asterisks above L_{tot} recording in Fig. 3), and the resulting changes in force were recorded (Fig. 6, *A* and *B*). V_{US} (in L_F s^{-1}) was obtained from the absolute value of the linear least-squares regression slope of length change versus slack time (Fig. 6 *C*) as described previously (Chase and Kushmerick, 1988; Chase et al., 1993). Control V_{US} (♦ in Fig. 7) was 3.3 ± 0.7 L_F s^{-1} (mean ± SD; $N = 29$; determinations were not made on two fibers), and the corresponding intercept on the ordinate was 4.1 ± 1.3% L_F (mean ± SD; $N = 29$; determinations were not made on two fibers).

For one fiber, maximal velocity of shortening (V_{max}) was determined from records obtained during isotonic shortening (load clamps) as described previously (Chase and Kushmerick, 1988). In this case, estimates of V_{max} were obtained by nonlinear least-squares regression fits of Hill's (1938) hyperbolic relation to force-velocity data.

For comparison between fibers, both V_{US} and V_{max} obtained at elevated η/η_0 were normalized to the average of bracketing control determinations (♦ in Fig. 7; also see Fig. 3). Results obtained using isotonic shortening were similar to those obtained by the slack method applied to the same fiber.

Strain-rate dependence of elastic modulus

To characterize the passive, viscous resistance to sarcomere motion, we used a method previously described by Brenner et al. (1986) and by Schoenberg (1988), as adopted in our laboratory (Chase et al., 1994a). In four fibers, small-amplitude ramp stretches (<0.5% L_F) were applied to relaxed (pCa > 8) fibers, and the resulting changes in force and L_S were recorded, as illustrated previously (Chase et al., 1994a). Linear least-squares regression was used to obtain slopes for both force (F) and L_S signals against time (dF/dt and dL_S/dt, respectively). The strain rate (dL_S/dt) was varied from 1.2×10^0 to 3.8×10^4 nm per half-sarcomere per second (nm $h.s.^{-1}$ s^{-1}). dL_S/dt for these measurements was obtained from the Schottky photodetector signal because of its wider bandwidth. Elastic modulus (K) was taken as the ratio $K = (dF/dt)/((dL_S/dt)/L_S)$. Individual measurements of K from all fibers were combined, binned by dL_S/dt (four to eight individual measurements per bin), and both K and dL_S/dt were averaged within each bin.

Determination of rate of isometric tension redevelopment

Kinetics of isometric tension redevelopment (k_{TR}) were determined in six fibers as described (Chase et al., 1994b; Regnier et al., 1996) using a protocol adapted from Brenner and Eisenberg (1986). k_{TR} was estimated from the half-time of tension recovery ($t_{0.5}$) by assuming a monoexponential relationship: $k_{TR} = \tau^{-1} = -\ln 0.5\ (t_{0.5})^{-1}$. k_{TR} estimated from $t_{0.5}$ was well correlated with that estimated from monoexponential fits to the data using nonlinear least-squares regression. The majority of k_{TR} data were obtained without L_S clamp, although the effect of viscosity on k_{TR} was similar in two of these same fibers comparing results with and without L_S control; our previous results (obtained using our methods of fiber preparation and stabilization) demonstrated that k_{TR} measured without L_S control was correlated with a paired measurement using L_S control in the same condition, although the latter was 20–30% faster (Chase et al., 1994b; Regnier et al., 1996). For comparison between fibers, k_{TR} was normalized to the average of bracketing control determinations (♦ in Fig. 9 *B*. Control k_{TR} was 9.1 ± 2.0 s^{-1} (mean ± SD; $N = 6$).

Statistical analysis

Statistical analysis, including linear and nonlinear least-squares regression, was performed using Excel (version 5.0a; Microsoft, Redmond, WA) or SigmaPlot for Windows (version 3.02; Jandel Scientific, San Rafael, CA). Statistical comparison of regression parameter estimates was carried out according to Draper and Smith (1981).

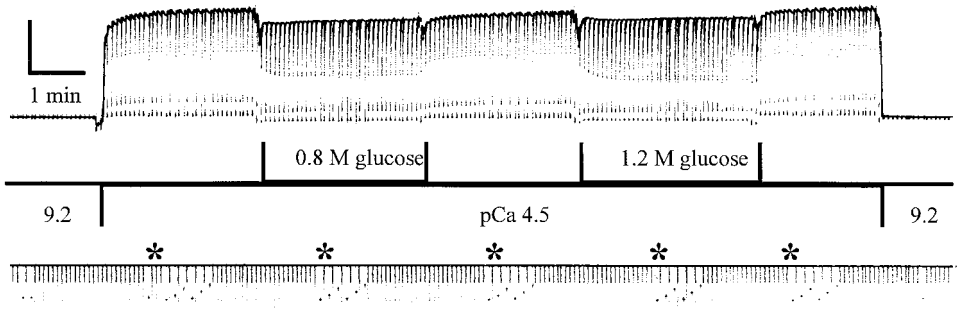

FIGURE 3 Chart recording (model RS4–5P, General Scanning, Watertown, MA) of force (*top*) and motor position (L_F; *bottom*) during a representative experiment. Solution pCa and added solutes are indicated by the central bar. Note that periods of high viscosity (0.8 M or 1.2 M glucose, which correspond to η/η_0 of approximately 1.5X or 2X, respectively) are bracketed by control solutions (no additional solute). Also note that the striation stabilization protocol resulted in periodic reductions in force to baseline (Materials and Methods). The start of each slack test is indicated by an asterisk above the L_F trace. Calibration bars correspond to 0.2 mN (upper force trace), 180 μm (lower L_F trace; isometric L_F was 1.51 mm), and 1 min (time).

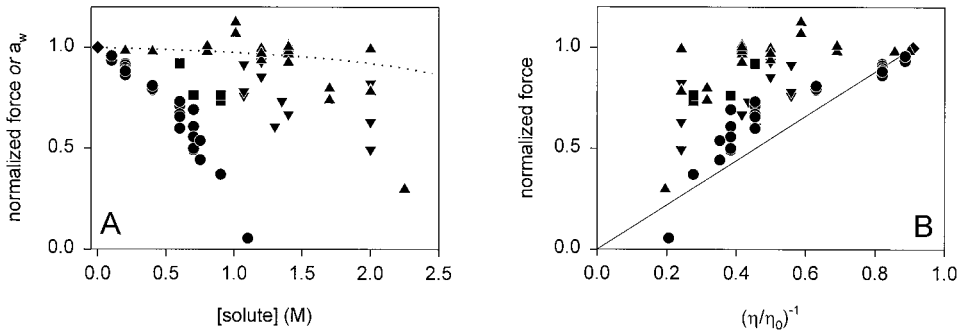

FIGURE 4 Relationship between maximal steady-state, Ca^{2+}-activated force (pCa 5.0–4.0) and (*A*) low MW sugar concentration or (*B*) solution viscosity. Symbols are the same as in Fig. 2. Points represent individual measurements normalized to the average of bracketing control measurements (◆). The dotted line in *A* corresponds to an estimate of a_w using data from Moore, 1972, and Weast, 1982 (see Results). In *B*, η/η_0 was estimated from the regressions shown in Fig. 2. Note that F_i was not strongly dependent on added solute, except for sucrose (●), or solution viscosity over the ranges studied.

RESULTS

Skinned fiber mechanics

Force

The effect of low MW sugars on maximal Ca^{2+}-activated isometric force was in many instances inhibitory, but the extent was variable (Fig. 4 *A*). The variability of the response of F_i to low MW sugars was not due to reduced Ca^{2+} sensitivity (Endo et al., 1979) as there was no effect of solution pCa, which was always <5. Inhibition of F_i was reversible (e.g., Fig. 3), and both F_i and sarcomere structure were stable during steady-state activation (Figs. 1 and 3). Sucrose appeared to be particularly inhibitory to F_i (Fig. 4, ●), although the cause of force inhibition by sucrose is not known. What is clear from the data is that viscosity is not a primary determinant of isometric force in the steady state (Fig. 4 *B*).

Because high concentrations of solutes were added to experimental solutions, we were concerned that observed physiological effects could be due to altered activity of water (a_w). We calculated a_w as a function of sucrose concentration from published data obtained at 20 and 50°C (Moore, 1972; Weast, 1982), and the result is plotted in Fig. 4 *A* (···). Note that little change in a_w is expected over the range of solute concentrations tested and thus is not likely responsible for effects of low MW sugars on fiber mechanics.

Added solutes readily permeated the filament lattice; thus there was no observed decrease in fiber diameter due to changes in osmotic pressure (Fig. 5). A slight increase in fiber diameter was observed when F_i was substantially inhibited by high sugar concentrations (Fig. 5). An increase in fiber diameter at low force would be expected from previous results that demonstrated that lattice spacing varied with Ca^{2+} activation level, and thus force, in the absence of high MW agents that compress the filament lattice (Brenner and Yu, 1985). Therefore, changes in force or other mechanical parameters could not be ascribed to altered filament lattice spacing.

Shortening velocity

As the greatest effect of viscosity is expected during motion (Eq. 1) and, although there is at most a small and variable effect of viscosity on F_i (Figs. 3 and 4), preliminary data suggested a greater effect of sucrose on velocity than on F_i (Chase and Kushmerick, 1988). Therefore we examined the effect of increased solution viscosity on the velocity of unloaded shortening (V_{US}). Superimposed, individual records from an experiment illustrate that, for a given extent of imposed shortening, the slack time is clearly longer at higher η/η_0 (compare slack times indicated by △ in Fig. 6, *B* versus *A*; also compare ▼ versus ◆ in Fig. 6 *C*), and thus V_{US} is slowed (Figs. 6 *C* and 7). Although there is slight curvature in the ΔL_F-time plot obtained at maximal Ca^{2+} activation (Fig. 6 *C*), as has been reported previously (Martyn et al., 1994; Metzger and Moss, 1988; Moss, 1986), it is evident from the data that slower V_{US} at increased η/η_0 did not result from the curvature as slowing is evident even at the earliest times examined.

Inhibition of maximal shortening velocity by low MW sugars is demonstrated in Fig. 7, which contains the combined data from 48 V_{US} measurements on 22 fibers. Obser-

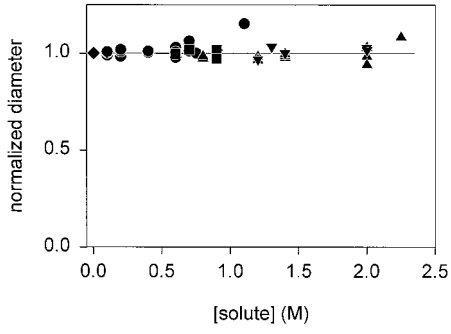

FIGURE 5 Lack of effect of low MW sugars on fiber diameter at maximal Ca^{2+} activation (pCa 5.0–4.0). Symbols are the same as in Fig. 2. Points represent individual measurements normalized to the average of bracketing control measurements (◆). The line was drawn according to $y = 1$.

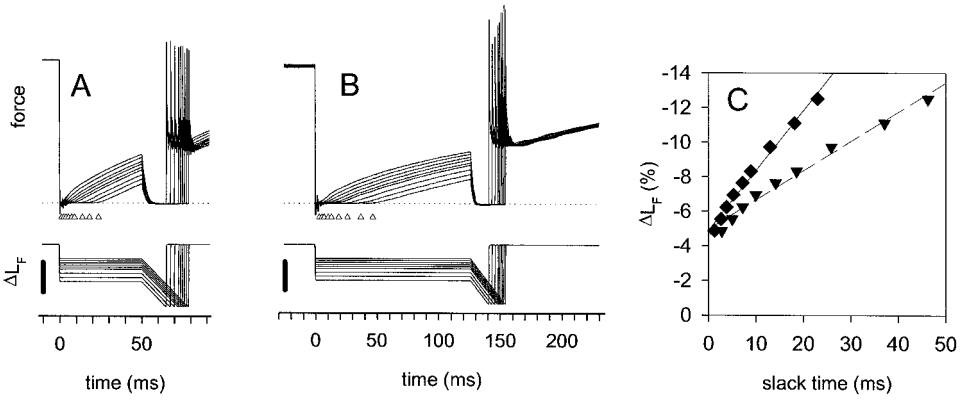

FIGURE 6 Determination of unloaded shortening velocity (V_{US}) in the absence (*A*) and presence (*B*) of 1.4 M fructose ($\eta/\eta_0 = 2.4$; Fig. 2) at maximal Ca^{2+} activation (pCa 4.0). Shown in panels *A* and *B* are nine superimposed force records (*top*) and corresponding L_F records (*bottom*) from two slack test protocols (as indicated by asterisks in Fig. 3). A total of 1024 points were digitized in each record (*A* and *B*) at 10 kHz (*A*) or 4 kHz (*B*). Force baseline is indicated by dotted lines (*A* and *B*, *top*). Measured slack times are indicated (△) below force records (*A* and *B*, *top*) and are plotted against corresponding ΔL_F (*C*). In *C*, the linear least squares regression estimates of V_{US} and intercept were 3.35 L_F s^{-1} and 5.0% L_F, respectively, for control measurements (—◆—; from data shown in *A*) and were 1.69 L_F s^{-1} and 5.0% L_F, respectively, for measurements in the presence of 1.4 M fructose (- - -▼- - -; from data shown in *B*). Force records were normalized to isometric steady-state force (*A* and *B*, *top*). Calibration bars (*A* and *B*, *bottom*) correspond to ΔL_F = 167 μm (10% L_F).

vations were excluded when $F_i < 0.7$ because V_{US} has previously been shown to co-vary with isometric steady-state force at varying degrees of Ca^{2+} activation (Martyn et al., 1994; Metzger and Moss, 1988) and also when fibers were activated with a constitutively activating troponin C, which enables force generation and sarcomere shortening in the absence (or presence) of calcium (Martyn et al., 1994). However, the conclusions of this work would remain unchanged if the excluded observations were retained in the data set. Also included in Figs. 7 are 3 measurements of V_{max} (○ and △), extrapolated from isotonic shortening data from one fiber in the presence of sucrose or glucose. It is evident that V_{max} was inhibited by addition of low MW sugars, similar to their effects on V_{US}; there was no detectable effect of low MW sugars on curvature of the force-velocity relation in these measurements. As with F_i, inhibition of V_{US} or V_{max} was fully reversible. Thus the observed reduction in shortening velocity was neither related to the method of determining the maximal velocity (V_{US} or V_{max}) nor was it a consequence of reduced isometric force; clearly, inhibition of shortening velocity is a direct result of addition of solute.

The data in Fig. 7 *A* appear to fall into two groups, distinguished between mono- and disaccharides (compare the two lines in Fig. 7 *A*), much like the bulk solution viscosity data shown in Fig. 2. When the data were replotted as a function of $(\eta/\eta_0)^{-1}$, as suggested by Eq. 1, the data for mono- and disaccharides converge to demonstrate that

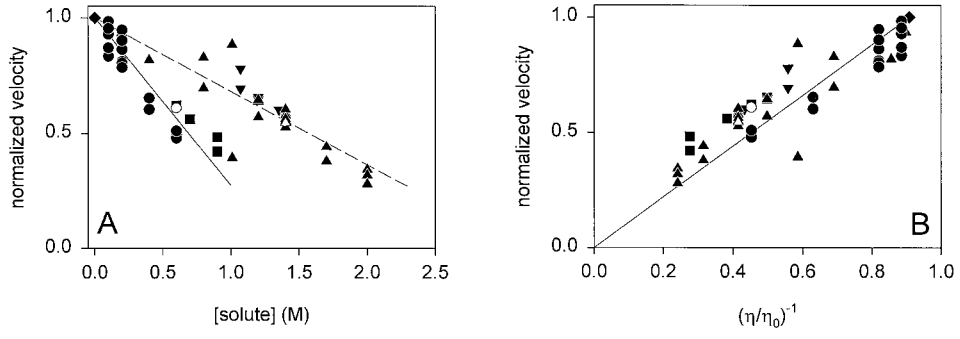

FIGURE 7 Relationship between unloaded shortening velocity (V_{US}; ●, ■, ▲, and ▼) or maximal velocity of shortening (V_{max}; ○ and △) at maximal Ca^{2+} activation (pCa 5.0–4.0) and (*A*) low MW sugar concentration or (*B*) solution viscosity. Symbols are the same as in Fig. 2 plus ○, sucrose, and △, glucose. Points represent individual measurements normalized to the average of bracketing control measurements (◆). Data are shown only for conditions in which F_i was greater than 70% of control (no added sugars) to eliminate possible bias as V_{US} is linearly proportional to isometric steady-state force, independent of method of activation (Martyn et al., 1994); applying this constraint resulted in exclusion of 14 observations although inclusion of these data did not statistically alter the conclusion (Results). The lines in *A* are the linear least-squares regressions on the data obtained in the presence of disaccharides (—) or monosaccharides (- - -), with each regression constrained to pass through the control point (x, y) = (0, 1). The line in *B* corresponds to $y = 1.1x$ and is thus constrained to pass through the control point (x, y) = (0.909, 1.0). Note the marked inverse dependence of shortening velocity on bulk solution viscosity illustrated in *B*.

shortening velocity decreases as viscosity increases (leftward on the abscissa of Fig. 7 *B*). As data from both mono- and disaccharides follow the same linear relationship (Fig. 7 *B*), we conclude that inhibition of shortening velocity is not a result of changes in solution properties, such as decreased a_w or increased osmolarity or osmotic pressure, but is a direct consequence of elevated viscosity.

Strain-rate dependence of elastic modulus

The simplest model to explain an effect of viscosity on fiber shortening velocity is to hypothesize a significant viscous force (relative to cross-bridge forces) that acts as a resistive load to impede filament sliding and thus to slow sarcomere shortening (Eq. 1). Previous calculations suggested that this possibility is unlikely (see Introduction). If this was in fact the mechanism underlying the results shown in Fig. 7, such a viscous load should be measurable in relaxed fibers as a viscosity-induced increase of elastic modulus at high strain rates (i.e., speeds of sarcomere stretch, dL_S/dt, comparable to V_{US}). Therefore, to test this hypothesis we measured the strain-rate dependence of elastic modulus (K; see Materials and Methods) of relaxed fibers at two viscosity levels: control ($\eta/\eta_0 = 1.1$) and $\eta/\eta_0 = 2.2$–2.4 (added [fructose] = 1.3–1.4 M).

Control measurements of the strain-rate dependence of K pooled from four relaxed fibers at 0.2 M $\Gamma/2$ (◆; Fig. 8) exhibited typical visco-elastic behavior as reported previously (Brenner et al., 1986; Chase et al., 1994a; Schoenberg, 1988). K increased at the fastest rates of stretch tested (particularly for $dL_S/dt > 10^3$ nm h.s.$^{-1}$ s^{-1}) with no evidence of saturation. Note that the magnitude of K was low over the range of dL_S/dt used because the measurements were made at physiological $\Gamma/2$, and thus the contribution of weak binding cross-bridges to the elastic modulus was minimal (Brenner et al., 1986; Schoenberg, 1988).

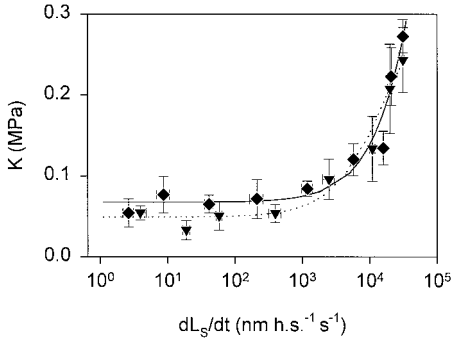

FIGURE 8 Lack of effect of increased solution viscosity on strain-rate dependence of elastic modulus (K) for four relaxed fibers (pCa > 8). Elastic moduli were measured using small-amplitude ramp stretches (Materials and Methods) and were obtained first in the absence (◆) and subsequently in the presence (▼) of 1.3–1.4 M fructose ($\eta/\eta_0 = 2.2$–2.4; Fig. 2). Changes in L_S were obtained from the output of a Schottky photodetector that indicated the position of a HeNe laser diffraction first order (Materials and Methods). Points are the mean ± SEM for four to eight observations. Lines are nonlinear least-squares regressions to the individual data points to

$$K = \beta_2\left(1 - e^{-\beta_1 \frac{dL_S}{dt}}\right) + \beta_0 \quad (5)$$

Note that the regression on the data obtained in the presence of fructose (· · ·▼· · ·) was not significantly different from that on the control data (—◆—).

There was no significant change in the relationship between K and dL_S/dt when η/η_0 was increased more than twofold (Fig. 8, ▼). The data obtained at elevated η/η_0 in fact tended to lie below control data, although this was within the noise of the measurements. What is most significant about these data is that there was no detectable effect of viscosity on the elastic modulus measured at rates of sarcomere length change comparable to V_{US} ($\sim 5 \times 10^3$ nm h.s.$^{-1}$ s^{-1}). Thus these observations are in agreement with previous predictions (Huxley, 1980) and measurements in intact (Bagni et al., 1995; Ford et al., 1977) and skinned frog fibers (Bagni et al., 1995) that viscous forces associated with filament sliding should be negligible. Therefore it became necessary to seek an alternate explanation for the effect of bulk solution viscosity on V_{US}.

Rate of tension redevelopment (k_{TR})

Examination of steady-state isometric force during maximal Ca^{2+} activation revealed at most a minor dependence on viscosity (Fig. 4 *B*). However, the approach to steady state as measured by k_{TR} was markedly dependent on η/η_0 (Fig. 9). As with V_{US}, k_{TR} in the six fibers tested decreased in proportion to $(\eta/\eta_0)^{-1}$, i.e., as η/η_0 increased (Fig. 9 *B*). Although L_S clamp was not used in these measurements (see Materials and Methods), k_{TR} was similarly slowed by elevated viscosity when the measurements were repeated using L_S clamp during tension recovery in two of these fibers (data not shown). We have previously reported that such paired measurements of k_{TR} obtained with and without L_S control are well correlated at varied degrees of Ca^{2+} activation in normal viscosity solutions (Chase et al., 1994b; Regnier et al., 1996). Thus the normalized data shown in Fig. 9 are representative of results obtained with or without L_S control. With or without L_S clamp, these measurements are made in conditions that are sarcomere isometric or nearly sarcomere isometric, respectively; even with filament elasticity within the sarcomere (Huxley et al., 1994), the rate of filament sliding is very slow during k_{TR} measurements. Thus these data (Fig. 9) are consistent with Fig. 8, illustrating that the predominant effect of bulk solution viscosity is on an aspect of actomyosin function other than imposing a resistive force that opposes filament sliding.

DISCUSSION

The major result of this study is that two kinetic measures of actomyosin mechanics within the intact sarcomere, i.e., the rate of isometric tension redevelopment (k_{TR}) and maximal

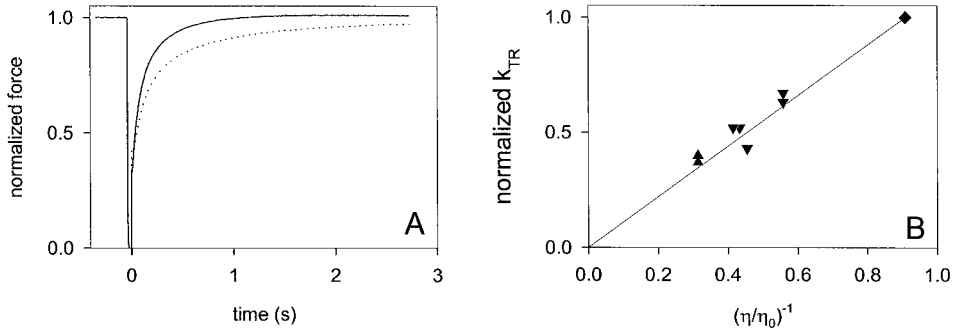

FIGURE 9 Relationship between the kinetics of tension redevelopment (k_{TR}) at maximal Ca^{2+} activation (pCa 4.0) and solution viscosity. (*A*) Two superimposed force records from the tension redevelopment protocol (see Materials and Methods) in the absence (—) or in the presence (· · ·) of 1.4 M fructose ($\eta/\eta_0 = 2.4$; Fig. 2). The k_{TR} estimated from $t_{1/2}$ measurements (Materials and Methods) was 7.8 s^{-1} (control) or 4.0 s^{-1} (1.4 M fructose). (*B*) Summary of data from six fibers. Symbols are the same as in Fig. 2. Points represent individual measurements normalized to the average of bracketing control measurements (◆). The line in *B* corresponds to $y = 1.1x$ (as in Fig. 7 *B*) and is thus constrained to pass through the control point $(x, y) = (0.909, 1.0)$. Note the marked inverse dependence of rate of tension redevelopment on bulk solution viscosity illustrated in *B*.

velocity of shortening (both V_{US} and V_{max}), were both markedly slowed when the solution viscosity was increased (Figs. 7 *B* and 9 *B*). There was a linear, inverse dependence of both kinetic parameters on solution viscosity (Figs. 7 *B* and 9 *B*) but not the concentration of solute used (Fig. 7 *A*) to vary viscosity; thus viscosity is the pertinent variable. The inverse dependence of kinetics on viscosity (Figs. 7 *B* and 9 *B*) strongly implies diffusional limitation(s) to those reactions. As slower kinetics were obtained for both isotonic and nearly-isometric conditions, we inferred that viscosity most likely affects the diffusional motion(s) of cross-bridges rather than filament sliding. Our results suggest that such diffusional motion(s) need to be more carefully considered in experimental design as well as in elucidating the mechanism of cross-bridge function.

Viscosity as a probe of muscle function

Beyond its utility in determining macromolecular size and shape, variation of solvent viscosity is a useful probe applied in studies of protein dynamics, ligand binding and reaction kinetics, and enzyme function (Ansari et al., 1992; Beece et al., 1980; Gavish and Werber, 1979; Hunt et al., 1994) but has been used very little in studies on muscle. The work reported here clearly demonstrates that viscosity directly impacts actomyosin kinetics as measured by V_{US} (Fig. 7 *B*) and k_{TR} (Fig. 9 *B*) in skinned muscle fibers. All of the reported effects of low MW sugars (used to vary viscosity) were reversible in these experiments; care was taken to ensure that structural and mechanical integrity of the fibers (Figs. 1 and 3) was maintained during the prolonged activations used to demonstrate reversibility and to ensure that measurements were obtained during steady-state conditions (Brenner, 1983; Chase and Kushmerick, 1988; Chase et al., 1994a,b; Sweeney et al., 1987). Previous reports that sucrose and glucose inhibit maximal Ca^{2+}-activated force (Ashley and Moisescu, 1977; Chase and Kushmerick, 1988; Endo et al., 1979) were confirmed here, although it appears likely that viscosity per se is not the relevant parameter for effects on F_i (Fig. 4). What is clear is that the observed effects occurred in the absence of osmotically induced changes in filament lattice spacing (as reflected by constant fiber diameter; Fig. 5), thus implying that changes in solute concentration were attained uniformly throughout the skinned fibers.

One of the practical considerations stemming from this work is that viscosity needs to be carefully considered in both the design of skinned fiber experiments and interpretation of experimental data. One such example is the inhibition of V_{US} when Dextran T-500 is added to fiber solutions (Metzger and Moss, 1987). High MW molecules like Dextran T-500 compress the filament lattice of skinned fibers and thus alter the geometry of cross-bridge attachment to actin, which is the most likely cause of decreased velocity. But Dextrans also increase the bulk solution viscosity (Materials and Methods). As the majority of Dextrans (average MW, 500,000) do not permeate the filament lattice (thus its utility for osmotic compression), the viscosity within the filament lattice does not increase to the same extent as the bulk solution. However, one must consider the minor fraction of Dextran that does permeate the lattice and thus alters viscosity within the fiber, providing a plausible, alternate explanation for the concentration-dependent inhibition of V_{US} by Dextran T-500 (Metzger and Moss, 1987).

A second practical implication of this work is the consideration of solution viscosity changes associated with variations in temperature. Although temperature clearly has direct effects on the thermodynamics and kinetics of biochemical processes, it also could have an additional, indirect effect on kinetics via its marked influence on the viscosity of water. For example, a temperature decrease from 25°C to 5°C results in a 71% increase in the viscosity of water (Weast, 1982), which would substantially affect V_{max} by itself (Fig. 7). Thus, effects of temperature on solution viscosity may be a significant component of temperature effects on chemomechanical kinetics.

Implications for limiting factors of muscle chemomechanical kinetics

There are several possible mechanisms by which low MW sugars could inhibit contractile function of skinned fibers. First, Parsegian et al. (1995) and Lumry (1995) point out cautions associated with osmotic stress at the molecular level and choice of solute or co-solvent in experiments of this type. Thus it is necessary to identify viscosity as the relevant effector, as was done here by using low MW (<400 MW), nonionic solutes having different dependencies of viscosity on concentration (Fig. 2). Second and most importantly, viscosity probes all molecular motions: 1) diffusion of substrate, products, and Ca^{2+}, 2) motions of the filaments, as in sarcomere shortening, 3) movement of myosin's motor domain to binding sites on the thin filament, and 4) subdomain motions within proteins including any that may be associated with changes in nucleotide state (e.g., nucleotide binding and hydrolysis as well as product dissociation) and with actin binding. In some experiments, the nonspecific nature of the probe may be a limitation, but as is the case in these experiments, there are also benefits to a general probe of protein dynamics. We can rule out the first possibility (diffusion of substrate, products, and Ca^{2+}) because the experiments were carried out during steady-state activation at saturating levels of Ca^{2+} and MgATP, and PCr and excess CK were included in the solutions which maintained MgADP in the micromolar range (Chase and Kushmerick, 1995). Even if this were not so, little or no effect on function would be expected for severalfold variation in Ca^{2+}, MgATP, or MgADP concentrations due to exacerbated diffusional gradients (Chase and Kushmerick, 1995). As described in Results, the second possibility is not relevant because similar slowing of kinetics was observed for both isotonic (V_{US} and V_{max}) and isometric (k_{TR}) measurements (Figs. 6, 7, and 9) and also because measurements indicated viscous resistance to filament sliding is minimal (Fig. 8). Below, we explore the implications of the remaining possibilities.

Kinetics of tension redevelopment and cross-bridge diffusion

Previous experiments demonstrated that the kinetics of tension redevelopment (k_{TR}) reflect different mechanisms at different levels of Ca^{2+} activation. At maximal Ca^{2+} activation, k_{TR} is dominated by the force-generating process of actomyosin interactions (Brenner and Eisenberg, 1986; Chase et al., 1994b; Metzger and Moss, 1990). In constrast, at submaximal Ca^{2+} activation, k_{TR} reflects the dynamic events within individual regulatory units (Chase et al., 1994b; Regnier et al., 1996). Because the results shown here were obtained at maximal Ca^{2+} activation, Fig. 9 therefore illustrates effects of viscosity on dynamic properties of the motor proteins rather than regulation.

Our conclusion that increased viscosity slows k_{TR} via an effect on cross-bridge diffusion to binding sites on actin (recall that the diffusion coefficient D of a sphere of radius r is $D = kT/6\pi\eta r$, where k is Boltzmann's constant and T is absolute temperature) implies in turn that cross-bridge diffusion is a limiting factor in determining the rate of tension development. Such a mechanism is implicit in the hypothesis of how phosphorylation of skeletal myosin light chain 2 (MLC_2) enhances k_{TR} (Metzger et al., 1989; Sweeney et al., 1993; Sweeney and Stull, 1990). Phosphorylation of MLC_2 is thought to bias the average position of cross-bridges away from the thick filament and thus closer to binding sites on actin (Levine et al., 1996), yielding a shorter average diffusion distance and faster tension redevelopment compared with cross-bridges having unphosphorylated MLC_2. According to this hypothesis, both phosphorylation of MLC_2 and viscosity should affect primarily the rate at which steady state is attained and, to a lesser extent, the steady-state force itself; this prediction is in accord with the data (Figs. 4 and 9) (Metzger et al., 1989; Sweeney et al., 1993; Sweeney and Stull, 1990). However, the kinetic influence of motor diffusion to its binding site is rarely considered explicitly in models of motor protein function (Howard, 1996; Hunt et al., 1994).

Shortening velocity

Considering the similarity between viscosity effects on shortening velocity (Fig. 7 *B*) and k_{TR} (Fig. 9), it seems likely that cross-bridge diffusion is also a limiting factor for the kinetics of sarcomere shortening under saturating conditions of both nucleotide and Ca^{2+} concentrations. A model that describes how motor diffusion can limit maximal sliding speed was developed by Hunt et al. (1994) for the kinesin-microtubule system, although their result is generally applicable to myosin and actin. In their model,

$$\langle v \rangle_{max} = \frac{d}{t_0 + t_K} \tag{4}$$

where d is the distance between binding sites, t_0 is the refractory time (no filament sliding), and t_K is the average time for thermal fluctuations to stretch a spring of stiffness K by distance d. Viscosity dependence of $\langle v \rangle_{max}$ enters the relationship (Eq. 4) because t_K is proportional to η. Although t_0 is the predominant term in the denominator for individual myosin molecules at physiological substrate concentrations (Finer et al., 1994; Molloy et al., 1995), it would be expected to become small for an ensemble of cross-bridges, as in a muscle fiber, and would thus explain the observed inverse dependence of V_{US} on solution viscosity (Fig. 7 *B*).

The view that cross-bridge attachment rate is a major limiting factor to isotonic shortening stands in contrast to the hypothesis outlined in the Introduction (Huxley, 1957), i.e., that attached, negatively strained cross-bridges, and thus detachment rate, is the primary determinant of shortening velocity in the intact sarcomere. It does not seem likely that cross-bridge detachment would be diffusion lim-

ited (unless subtrate was limiting, which was not the case in these experiments). A possible explanation is that the limitation involves diffusional motions of the cross-bridge other than those associated with the initial binding to actin. It is also possible that the diffusional limitations of V_{US} and k_{TR} do not reflect the same processes. However, in the absence of evidence to the contrary, we consider the simplified view of only a single, common limiting process that can explain all of the data, diffusion of myosin heads to binding sites on actin, to be the more likely possibility.

If diffusion of cross-bridges to binding sites on actin is truly a kinetic constraint on shortening velocity, then that would imply only a small number of working cross-bridges are associated with an actin filament moving at V_{max} (Homsher et al., 1996; Spudich, 1994; Uyeda et al., 1990, 1991). Actin filament translocation by small numbers of cross-bridges could explain the observed gradation of V_{US} with activation level in skinned fibers (Martyn et al., 1994; Metzger and Moss, 1988; Moss, 1986) and also the Ca^{2+}-dependent gradation of sliding speed for regulated actin filaments in an in vitro motility assay (Gordon et al., 1997; Homsher et al., 1996). Such a low apparent duty ratio also seems likely from structural and theoretical considerations (Howard, 1997) and direct observations of individual myosin molecules at physiological substrate concentrations (Finer et al., 1994; Molloy et al., 1995).

In addition to the mechanistic significance of these observations, the 2- to 10-fold higher viscosity of myoplasm relative to water (Kushmerick and Podolsky, 1969; Sachs and Latorre, 1974) may at least in some instances have significant physiological implications. First, our data would predict that V_{max} should become faster when an intact muscle fiber is skinned. Furthermore, physiologically relevant variations in viscosity likely influence motility of ectotherms. In particular, certain species of fish may experience significant changes in temperature, with concomitant changes in cytoplasmic viscosity (see above) and thus changes in the speed and energy requirements for swimming (Moerland and Sidell, 1986).

CONCLUSIONS

Our results imply that viscosity is a generally useful probe of cross-bridge function within the structural constraints of the intact filament lattice. Additionally, viscosity needs to be carefully considered in experimental design and interpretation of skinned muscle fiber experiments. As both isometric (k_{TR}; Fig. 9 *B*) and isotonic (V_{US} and V_{max}; Fig. 7 *B*) contraction kinetics were slowed by elevated viscosity, we conclude that viscosity most likely affects the diffusional motion of cross-bridges to binding sites on actin, thus supporting the idea that cross-bridge dynamics are intimately linked to the kinetics of force generation (Thomas et al., 1995).

We thank Dr. T. W. Beck, Dr. Ying Chen, M. Mathiason, and R. Stuppard for excellent technical assistance; M. Bandy and D. Boster for assistance with figures; Drs. R. Horowits and J. W. Shriver for assistance with T-clips; Dr. T. S. Moerland for critical suggestions at an early stage of this investigation; and Dr. J. M. Metzger for comments on the manuscript.
This work was Supported by National Institutes of Health grants HL52558, AR36281, HL31962, and AM07783.

REFERENCES

Ansari, A., C. M. Jones, E. R. Henry, J. Hofrichter, and W. A. Eaton. 1992. The role of solvent viscosity in the dynamics of protein conformational changes. *Science.* 256:1796–1798.

Ashley, C. C., and D. G. Moisescu. 1977. Effect of changing the composition of the bathing solutions upon the isometric tension-pCa relationship in bundles of crustacean myofibrils. *J. Physiol.* 270:627–652.

Bagni, M. A., G. Cecchi, F. Colomo, and P. Garzella. 1995. Absence of mechanical evidence for attached weakly binding cross-bridges in frog relaxed muscle fibres. *J. Physiol.* 482:391–400.

Beece, D., L. Eisenstein, H. Frauenfelder, D. Good, M. C. Marden, L. Reinisch, A. H. Reynolds, L. B. Sorensen, and K. T. Yue. 1980. Solvent viscosity and protein dynamics. *Biochemistry.* 19:5147–5157.

Brenner, B. 1983. Technique for stabilizing the striation pattern in maximally calcium-activated skinned rabbit psoas fibers. *Biophys. J.* 41: 99–102.

Brenner, B., J. M. Chalovich, L. E. Greene, E. Eisenberg, and M. Schoenberg. 1986. Stiffness of skinned rabbit psoas fibers in MgATP and MgPPi solution. *Biophys. J.* 50:685–691.

Brenner, B., and E. Eisenberg. 1986. Rate of force generation in muscle: correlation with actomyosin ATPase activity in solution. *Proc. Natl. Acad. Sci. USA.* 83:3542–3546.

Brenner, B., and L. C. Yu. 1985. Equitorial x-ray diffraction from single skinned rabbit psoas fibers at various degrees of activation. *Biophys. J.* 48:829–834.

Burton, K., and A. F. Huxley. 1995. Identification of source of oscillations in apparent sarcomere length measured by laser diffraction. *Biophys. J.* 68:2429–2443.

Chase, P. B., T. M. Denkinger, and M. J. Kushmerick. 1996. Effect of solution viscosity on calcium activated, skinned skeletal muscle fibers. *Biophys. J.* 70:A41.

Chase, P. B., and M. J. Kushmerick. 1988. Effects of pH on contraction of rabbit fast and slow skeletal muscle fibers. *Biophys. J.* 53:935–946.

Chase, P. B., and M. J. Kushmerick. 1995. Effect of physiological ADP levels on contraction of single skinned fibers from rabbit fast and slow muscles. *Am. J. Physiol*. 268:C480–C489.

Chase, P. B., D. A. Martyn, and J. D. Hannon. 1994a. Activation dependence and kinetics of force and stiffness inhibition by aluminiofluoride, a slowly dissociating analogue of inorganic phosphate, in chemically skinned fibres from rabbit psoas muscle. *J. Muscle Res. Cell Motil.* 15:119–129.

Chase, P. B., D. A. Martyn, and J. D. Hannon. 1994b. Isometric force redevelopment of skinned muscle fibers from rabbit with and without Ca^{2+}. *Biophys. J.* 67:1994–2001.

Chase, P. B., D. A. Martyn, M. J. Kushmerick, and A. M. Gordon. 1993. Effects of inorganic phosphate analogues on stiffness and unloaded shortening of skinned muscle fibres from rabbit. *J. Physiol.* 460: 231–246.

Cooke, R. 1995. The actomyosin engine. *FASEB J.* 9:636–642.

Draper, N. R., and H. Smith. 1981. Applied Regression Analysis. John Wiley and Sons, New York. 709 pp.

Edman, K. A. P. 1979. The velocity of unloaded shortening and its relation to sarcomere length and isometric force in vertebrate muscle fibres. *J. Physiol.* 291:143–159.

Endo, M., T. Kitazawa, M. Iino, and Y. Kakuta. 1979. Effect of "viscosity" of the medium on mechanical properties of skinned skeletal muscle fibers. *In* Cross-Bridge Mechanism in Muscle Contraction. University of Tokyo Press, Tokyo. 365–374.

Finer, J. T., R. M. Simmons, and J. A. Spudich. 1994. Single myosin molecule mechanics: piconewton forces and nanometre steps. *Nature.* 368:113–119.

Fisher, A. J., C. A. Smith, J. B. Thoden, R. Smith, K. Sutoh, H. M. Holden, and I. Rayment. 1995. X-ray structures of the myosin motor domain of *Dictyostelium discoideum* complexed with MgADP·BeF_x and MgADP·AlF4$^-$. *Biochemistry.* 34:8960–8972.

Ford, L. E., A. F. Huxley, and R. M. Simmons. 1977. Tension responses to sudden length change in stimulated frog muscle fibres near slack length. *J. Physiol.* 269:441–515.

Gasser, H. S., and A. V. Hill. 1924. The dynamics of muscular contraction. *Proc. R. Soc. Lond. B.* B96:398–437.

Gavish, B., and M. M. Werber. 1979. Viscosity-dependent structural fluctuations in enzyme catalysis. *Biochemistry.* 18:1269–75.

Goldman, Y. E. 1987. Measurement of sarcomere shortening in skinned fibers from frog muscle by white light diffraction. *Biophys. J.* 52:57–68.

Gordon, A. M., M. LaMadrid, Y. Chen, Z. Luo, and P. B. Chase. 1997. Calcium regulation of skeletal muscle thin filament motility in vitro. *Biophys. J.* 72:1295–1307.

Harford, J. J., and J. M. Squire. 1992. Evidence for structurally different attached states of myosin cross-bridges on actin during contraction of fish muscle. *Biophys. J.* 63:387–396.

Hill, A. V. 1938. The heat of shortening and the dynamic constants of muscle. *Proc. R. Soc. Lond. B.* 126:136–195.

Homsher, E., B. Kim, A. Bobkova, and L. S. Tobacman. 1996. Calcium regulation of thin filament movement in an in vitro motility assay. *Biophys. J.* 70:1881–1892.

Howard, J. 1997. Molecular motors: structural adaptations to cellular functions. *Nature.* 389:561–567.

Howard, J. 1996. The movement of kinesin along microtubules. *Annu. Rev. Physiol.* 58:703–729.

Hunt, A. J., F. Gittes, and J. Howard. 1994. The force exerted by a single kinesin molecule against a viscous load. *Biophys. J.* 67:766–781.

Huxley, A. 1980. Reflections on Muscle. Princeton University Press, Princeton, NJ. 111 pp.

Huxley, A. F. 1957. Muscle structure and theories of contraction. *Prog. Biophys.* 7:255–318.

Huxley, A. F., and R. M. Simmons. 1971. Proposed mechanism of force generation in striated muscle. *Nature.* 233:533–538.

Huxley, H. E. 1969. The mechanism of muscular contraction. *Science.* 164:1356–1366.

Huxley, H. E., A. Stewart, H. Sosa, and T. Irving. 1994. X-ray diffraction measurements of the extensibility of actin and myosin filaments in contracting muscle. *Biophys. J.* 67:2411–2421.

Iwazumi, T., and G. H. Pollack. 1979. On-line measurement of sarcomere length from diffraction patterns in muscle. *IEEE Trans. Biomed. Engr.* 26:86–93.

Kushmerick, M. J., and R. J. Podolsky. 1969. Ionic mobility in muscle cells. *Science.* 166:1297–1298.

Levine, R. J. C., R. W. Kensler, Z. Yang, J. T. Stull, and H. L. Sweeney. 1996. Myosin light chain phosphorylation affects the structure of rabbit skeletal muscle thick filaments. *Biophys. J.* 71:898–907.

Lumry, R. 1995. On the interpretation of data from isothermal processes. *Methods Enzymol.* 259:628–720.

Martyn, D. A., P. B. Chase, J. D. Hannon, L. L. Huntsman, M. J. Kushmerick, and A. M. Gordon. 1994. Unloaded shortening of skinned muscle fibers from rabbit activated with and without Ca^{2+}. *Biophys. J.* 67:1984–1993.

McKie, J. E., and J. F. Brandts. 1972. High precision capillary viscometry. *Methods Enzymol.* 26:257–288.

Metzger, J. M., M. L. Greaser, and R. L. Moss. 1989. Variations in cross-bridge attachment rate and tension with phosphorylation of myosin in mammalian skinned skeletal muscle fibers: implications for twitch potentiation in intact muscle. *J. Gen. Physiol.* 93:855–883.

Metzger, J. M., and R. L. Moss. 1987. Shortening velocity in skinned single muscle fibers: influence of filament lattice spacing. *Biophys. J.* 52:127–131.

Metzger, J. M., and R. L. Moss. 1988. Thin filament regulation of shortening velocity in rat skinned skeletal muscle: effects of osmotic compression. *J. Physiol.* 398:165–175.

Metzger, J. M., and R. L. Moss. 1990. Calcium-sensitive cross-bridge transitions in mammalian fast and slow skeletal muscle fibers. *Science.* 247:1088–1090.

Moerland, T. S., and B. D. Sidell. 1986. Contractile responses to temperature in the locomotory musculature of striped bass *Morone saxatilis*. *J. Exp. Zool.* 240:25–33.

Molloy, J. E., J. E. Burns, J. Kendrick-Jones, R. T. Tregear, and D. C. S. White. 1995. Movement and force produced by a single myosin head. *Nature.* 378:209–212.

Moore, W. J. 1972. Physical Chemistry. Prentice-Hall, Englewood Cliffs, NJ.

Moss, R. L. 1986. Effects on shortening velocity of rabbit skeletal muscle due to variations in the level of thin-filament activation. *J. Physiol.* 377:487–505.

Parsegian, V. A., R. P. Rand, and D. C. Rau. 1995. Macromolecules and water: probing with osmotic stress. *Methods Enzymol.* 259:43–94.

Regnier, M., D. A. Martyn, and P. B. Chase. 1996. Calmidazolium alters Ca^{2+} regulation of tension redevelopment rate in skinned skeletal muscle. *Biophys. J.* 71:2786–2794.

Rüdel, R., and F. Zite-Ferenczy. 1979. Do laser diffraction studies on striated muscle indicate stepwise sarcomere shortening? *Nature.* 278: 573–575.

Sachs, F., and R. Latorre. 1974. Cytoplasmic solvent structure of single barnacle muscle cells studied by electron spin resonance. *Biophys. J.* 14:316–326.

Schoenberg, M. 1988. Characterization of the myosin adenosine triphosphate (M·ATP) crossbridge in rabbit and frog skeletal muscle fibers. *Biophys. J.* 54:135–148.

Spudich, J. A. 1994. How molecular motors work. *Nature.* 372:515–518.

Sweeney, H. L., B. F. Bowman, and J. T. Stull. 1993. Myosin light chain phosphorylation in vertebrate striated muscle: regulation and function. *Am. J. Physiol*. 264:C1085–C1095.

Sweeney, H. L., S. A. Corteselli, and M. J. Kushmerick. 1987. Measurements on permeabilized skeletal muscle fibers during continuous activation. *Am. J. Physiol*. 252:C575–C580.

Sweeney, H. L., and J. T. Stull. 1990. Alteration of cross-bridge kinetics by myosin light chain phosphorylation in rabbit skeletal muscle: implications for regulation of actin-myosin interaction. *Proc. Natl. Acad. Sci. USA.* 87:414–418.

Thomas, D. D., S. Ramachandran, O. Roopnarine, D. W. Hayden, and E. M. Ostap. 1995. The mechanism of force generation in myosin: a disorder-to-order transition, coupled to internal structural changes. *Biophys. J.* 68:135S–141S.

Uyeda, T. Q. P., S. J. Kron, and J. A. Spudich. 1990. Myosin step size estimation from slow sliding movement of actin over low densities of heavy meromyosin. *J. Mol. Biol.* 214:699–710.

Uyeda, T. Q. P., H. M. Warrick, S. J. Kron, and J. A. Spudich. 1991. Quantized velocities at low myosin densities in an in vitro motility assay. *Nature.* 352:307–311.

Weast, R. C. 1982. CRC Handbook of Chemistry and Physics. CRC Press, Boca Raton, FL.

Yu, L., and B. Brenner. 1989. Structures of actomyosin crossbridges in relaxed and rigor muscle fibers. *Biophys. J.* 55:441–453.